ACS OMEGA

Article

Cite This: ACS Omega 2019, 4, 1375−1385

http://pubs.acs.org/journal/acsodf

Establishing Cost-Effective Computational Models for the Prediction of Lanthanoid Binding in $[Ln(NO_3)]^{2+}$ (with Ln = La to Lu)

Charles C. Peterson,[†,‡] Deborah A. Penchoff,[*,‡] John D. Auxier, II,[§] and Howard L. Hall[*,‡,∥,§,⊥]

[†]Research Information Technology Services, University of North Texas, 225 S. Avenue B, Denton, Texas 76201, United States

[‡]Institute for Nuclear Security, University of Tennessee, 1640 Cumberland Avenue, Knoxville, Tennessee 37996, United States

[§]Department of Nuclear Engineering, University of Tennessee, 301 Middle Dr., Pasqua Nuclear Engineering Bldg., Knoxville, Tennessee 37996, United States

[∥]Radiochemistry Center of Excellence (RCOE), University of Tennessee, 1508 Middle Dr., Ferris Hall, Knoxville, Tennessee 37996, United States

[⊥]Y-12 National Security Complex, Oak Ridge, Tennessee 37830, United States

Supporting Information

ABSTRACT: Evaluating the efficiency of predictive methods is critical to the processes of upscaling laboratory processes to full-scale operations on an industrial scale. With regard to separation of lanthanoids, there is a considerable motivation to optimize these processes because of immediate use in nuclear fuel cycle operations, nuclear forensics applications, and rare-earth metal recovery. Efficient predictive capabilities in Gibbs free energies of reaction are essential to optimize separations and ligand design for selective binding needed for various radiochemical applications such as nuclear fuel disposition and recycling of lanthanoid fission products into useful radioisotope products. Ligand design is essential for selective binding of lanthanoids, as separating contiguous lanthanoids is challenging because of the similar behavior these elements exhibit. Modeling including electronic structure calculations of lanthanoid-containing compounds is particularly challenging because of the associated computational cost encountered with the number of electrons correlated in these systems and relativistic considerations. This study evaluates the predictive capabilities of various ab initio methods in the calculation of Gibbs free energies of reaction for $[Ln(NO_3)]^{2+}$ compounds (with Ln = La to Lu), as nitrates are critical in traditional separation processes utilizing nitric acid. The composite methodologies evaluated predict Gibbs free energies of reaction for $[Ln(NO_3)]^{2+}$ compounds within 5 kcal mol^{-1} in most cases from the target method [CCSD(T)-FSII/cc-pwCV∞Z-DK3+SO] at a fraction of the computational cost.

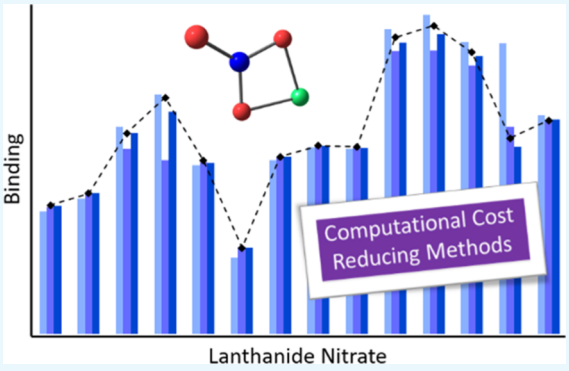

INTRODUCTION

Nuclear operations involve handling of fission products (many of which are lanthanoids) and the partitioning for inclusion for other industrial processes such as radioisotope source production, nuclear forensics measurements, or waste disposition. Efficient and cost-effective methods of partitioning fission products into useful waste or product streams require specialized chemical processes that are well-suited for these unique applications. Development of these processes to separate fission products also requires careful selection of ligands to selectively extract useful elements (such as rare-earth metals) from bulk materials. These ligands are often selected based on radiation tolerance because degradation of chemical components from irradiation may result in a decrease of process efficiency.[1] Design of selective ligands to optimize separation processes often involves hazardous experiments that could greatly benefit from additional information regarding the suitability of a given ligand. Furthermore, lanthanoids are often used as surrogates for complexation and structural analysis of actinoid compounds as it was recently highlighted in a study by Corbey and co-workers for americium compounds.[2]

Although there have been many advances in separation science, efficient and highly selective binding to lanthanoids and actinoids continues to be present challenges.[3,4] Consequently, developing effective computational protocols to model lanthanoid-binding characteristics can aid researchers in nuclear operations to design new and improved methods of separating lanthanoids from bulk materials. Traditional electronic structure modeling of lanthanoid-containing compounds can be computationally expensive and inefficient for rapid predictive capabilities of large fully complexed compounds. Increasing the efficiency of these methods can provide

Received: September 16, 2018
Accepted: December 12, 2018
Published: January 16, 2019

DOI: 10.1021/acsomega.8b02403
ACS Omega 2019, 4, 1375−1385

a means of further optimizing chemical processes while providing guidance in laboratory experiments (i.e., preselection of potentially efficient ligands) without requiring the use of extensive computational resources, thus providing tools to optimize separation processes to a wider segment of the community. Benchtop chemical processes are often focused on determining if a particular method is possible and less on the efficiency of the chemical process. Although this is adequate for exploratory laboratory exercises, the question of efficiency in upscaling must be considered for any wide adoption of a process. To this end, determination of the thermochemical characteristics and prediction of how these may affect larger industrial processes is a significant consideration. Providing engineers with predictive capabilities to perform low-cost (both computationally and monetarily) simulations of complex lanthanoid systems and predictions of separation efficiency reduce the overall cost of industrial process design. Cost reduction stems from the ability to prototype systems in a virtual environment such that primary and alternate designs may be evaluated for further, often costlier, exploration.[5]

Among electronic structure methods in computational modeling, density functional theory (DFT) methods have been widely used to describe the thermochemical properties of lanthanoid-containing compounds. DFT can describe electron correlation at a reasonable computational cost; however, the predicted thermochemical characteristics can be largely dependent on the choice of level of theory as it was recently shown in a systematic study of 5f elements in an actinoid nitrate study.[6] Furthermore, ab initio[7] and composite methods[8] have been used for thermochemical predictions, but these methodologies vary in computational cost and accuracy. Utilizing ab initio methods for lanthanoid-containing compounds can be challenging because of the number of electrons and basis functions needed to describe these systems, which increase the computational cost. Composite methods, such as *f*-ccCA[9] (which follows the correlation consistent Composite Approach, ccCA, methodology[10,11]) and Feller−Peterson−Dixon (FPD),[12] have been developed to describe the thermochemical properties of lanthanoid systems with the accuracy of methods such as coupled cluster with perturbative doubles and triples [CCSD(T)] at a lower computational cost. Both of these methods describe dynamical electron correlation, outer-core electron correlation, and effects due to special relativity including spin−orbit (SO) coupling. There have also been studies which utilized ab initio methods for thermochemical[9,13] and spectroscopic[13] analysis of small lanthanoid compounds.

Establishing accurate and cost-effective predictive computational models for selective binding of lanthanoids and actinoids is essential for the optimization and design of separations agents; and as previously indicated, reliable predictive capabilities for lanthanoid compounds are not only needed for fission products but also as surrogates for actinoid studies. Large systematic analysis of lanthanoid-containing complexes performed with ab initio methods can become highly restricted by the size of the compounds because of the computational constraints. This study focuses on lanthanoid mononitrate as this is a highly important system in lanthanoid- and actinoid-separation because of the common binding of one or more nitrates stemming from the often use of nitric acid in the separation process[14,15]—as also noted by Glatz in cataloguing all of the industrial processing for handling spent nuclear fuel.[16] Because of the presence of nitric acid, nitrates bound to lanthanoids and actinoids have been observed in multiple separations, and synthesis and characterization studies with bis[(phosphino)methyl]pyridine-1-oxide (NOPOPO),[2] 1,2-phenylenediphosphonates,[17] 2,6-bis[(diphenylphosphino)-methyl]pyridine *N*,*P*,*P*′-trioxide,[18] 2-((diphenylphosphino) methyl)pyridine, dioxide and 2,6-bis((diphenylphosphino)-methyl)pyridineiV,*P*,*P*′-trioxide,[19] decorated pyridine and pyridine *n*-oxide platforms,[3] tetra-n-donor extractants,[20] undiluted quaternary ammonium ionic liquid,[21] cyclic dilactams,[22] bis-1,2,3-triazolebipyridine,[23] and cyclic imide dioximes,[24] among others.

This work evaluates the performance of ab initio methodologies including MP2 and CCSD(T) calculations, along with composite methods to predict the Gibbs free energy of reaction involving the binding of nitrates to lanthanoid ions across the lanthanoid series (namely $[Ln(NO_3)]^{2+}$, with Ln = La to Lu). Additionally, the proposed method A and method B (as described in the Methods section) are evaluated for the prediction of Gibbs free energies of reaction of $[Ln(OH)]^{2+}$. The $[Ln(OH)]^{2+}$ model system is chosen as a secondary test set for the proposed methods because of hydroxyl anions bound to lanthanoids being important in separations of lanthanoids and actinoids, as illustrated in separations of americium from lanthanoids.[25]

METHODS

The ab initio methods, MP2[26,27] and CCSD(T),[27] are used to calculate the Gibbs free energies of reaction of $[Ln(NO_3)]^{2+}$ (where Ln = La−Lu). These methods are also used to determine the accuracy of the composite methodologies utilized in this study. Correlation-consistent basis sets are used throughout this study. The cc-pVnZ-DK3[12] basis set is used for the lanthanoids, whereas cc-pVnZ-DK[28] is used for the N and O atoms (where $n = \zeta$ level). Also, the weighted core valence (cc-pwCVnZ-DK3 for Ln atoms; cc-pCVnZ-DK for N and O atoms)[12,28] is used when accounting for core correlation. The third-order Douglas−Kroll−Hess Hamiltonian[29] is used to describe scalar relativistic effects.

The model reaction for this study is described by eq 1.

$$Ln^{3+}_{(g)} + NO_3^-{}_{(g)} \rightarrow [Ln(NO_3)]^{2+}_{(g)} \quad (1)$$

Six ab initio methods are used to compute Gibbs free energies of the reaction of $[Ln(NO_3)]^{2+}$ compounds [with Ln = La−Lu]. These methods are CCSD(T)-FSI/cc-pVTZ-DK3, MP2-FSI/cc-pVTZ-DK3, CCSD(T)-FSII/cc-pwCVTZ-DK3, MP2-FSI/cc-pV∞Z-DK3, CCSD(T)-FSI/cc-pV∞Z-DK3, and CCSD(T)-FSII/cc-pwCV∞Z-DK3. The description of the correlation space is indicated with the "FS" labels (for "frozen shell"), with FSI and FSII referring to the electrons in the correlation space. The FSI calculations include the valence electrons in the correlation space (4f5s5p for Ln atoms and 2s2p for N and O atoms). The FSII calculations add the outer-core electrons (FSI + 4s4p4d for Ln atoms and FSI + 1s for N and O atoms). The cc-pV∞Z-DK3 cc-pwCV∞Z-DK3 refers to the basis sets used to calculate at the complete basis set (CBS)[8] limit. For the CBS calculations, the Hartree−Fock extrapolations use a two-point formula developed by Karton and Martin,[30] described by eq 2

$$E_n = E_{CBS} + A(n+1)e^{-6.57\sqrt{n}} \quad (2)$$

where n is 3 and 4 for triple- and quadruple-ζ basis sets (cc-pVTZ-DK3 and cc-pVQZ-DK3),[12,28] respectively. The corre-

DOI: 10.1021/acsomega.8b02403
ACS Omega 2019, 4, 1375−1385

lation energy is extrapolated using a two-point extrapolation formula[31] described by eq 3, with n = 2 and 3 (as utilized by Lu and Peterson[12] for lanthanoid-containing systems).

$$E_n = E_{CBS} + A(n + 1/2)^{-4} \quad (3)$$

The accuracy of predictive capabilities of these methods is evaluated with respect to CCSD(T)-FSII/cc-pwCV∞Z-DK3 (i.e., target method included in this study) as it contains the highest amount of dynamic electronic correlation, outer-core correlation, and extrapolation to the CBS limit.

Various composite schemes have also been utilized, including *f*-ccCA[9] and newly proposed variations (method A and method B). The total energy described by *f*-ccCA[9] is shown by eq 4.

$$E_{total} = E_{ref}(MP2) + \Delta E_{CC}(CCSD(T)) + \Delta E_{CV}(CCSD(T)) + \Delta E_{spin} \quad (4)$$

The reference energy (E_{ref}) is described by MP2-FSI/cc-pV∞Z-DK3. The ΔE_{cc} term describes higher dynamic electronic correlation from CCSD(T)-FSI/cc-pVTZ-DK3. The ΔE_{CV} term describes the electronic correlation from the outer-core electronic correlation from CCSD(T)-FSII/cc-pwCVTZ-DK3. The ΔE_{spin} term describes the SO interactions from the four-component Dirac−Hartree−Fock and triple-ζ basis set developed by Dyall,[32] and it is calculated as shown in previous work.[33]

Another composite scheme, similar to *f*-ccCA[9] except that the ΔE_{spin} term is removed, is shown by eq 5. This composite method is referred throughout this article as method A.

$$E_{total} = E_{ref}(MP2) + \Delta E_{CC}(CCSD(T)) + \Delta E_{CV}(CCSD(T)) \quad (5)$$

Last, the composite scheme described by eq 6 removes the ΔE_{CC} term and utilizes CCSD(T)-FSI/cc-pV∞Z-DK3 in the reference energy (instead of MP2). This composite method is referred to as method B throughout this article.

$$E_{total} = E_{ref}(CCSD(T)) + \Delta E_{CV}(CCSD(T)) \quad (6)$$

The Gibbs free energy for the proposed reaction (ΔG_{rxn}) for eq 1 is calculated as shown in eq 7, with the total energy obtained with the methods described in eqs 4−6, and thermochemical corrections obtained with DFT at 298.15 K (for the optimized structures as indicated in the Methods section). This approach was recently utilized in a similar study of $[An(NO_3)]^{2+}$ compounds, for which the thermochemical corrections for the Gibbs free energies of reaction are obtained at each level of theory utilized for the geometry and vibrational frequency calculations.[6]

$$\Delta G_{rxn(g)} = \Delta G[[Ln(NO_3)]^{2+}{}_{(g)}] - \Delta G[Ln^{3+}{}_{(g)}] - \Delta G[NO_3^{-}{}_{(g)}] \quad (7)$$

Although the focus of this study is on nitrate binding to lanthanoids, methods A and B are also evaluated against the target methodology for Gibbs free energies of reaction for hydroxyl anion binding to lanthanoids (namely $[Ln(OH)]^{2+}$) for method-verification purposes.

The geometry optimizations are performed utilizing DFT following a protocol in previous work,[34] with the B3LYP[35,36] functional, the Stuttgart RSC Segmented ECP and associated basis set for the lanthanoid atoms, and the 6-311++G**[37] basis set for O and N atoms with tight tolerances and extra fine grid. The ECP accounts for scalar relativistic effects by replacing 28 electrons with a relativistic pseudopotential. The compounds are optimized without imposing symmetry constraints. Thermochemical corrections are calculated at 298.15 K. No imaginary frequencies were found. The geometry optimizations and vibrational frequency calculations calculated with the B3LYP functional are obtained with the NWChem 6.8 package.[38] All single-point calculations (except for Dirac−Hartree−Fock) are performed with MOLPRO2015.[39] The DIRAC16[40] software package was used for Dirac−Hartree−Fock calculations. Basis sets for non-lanthanoids are obtained from the Environmental Molecular Sciences Laboratory (EMSL) database.[41,42]

RESULTS AND DISCUSSION

Unless otherwise indicated, the results discussed in this section correspond to an Ln IV configuration in the gas phase. This notation follows the NIST Atomic Spectra Database spectra name classifications which correspond to a defined electronic structure associated with each state, as shown in Table 1.[43]

Table 1. Electronic Configuration for Ln IV and Ln III[43]

Ln	Ln IV	Ln III
La	[Cd]$5p^6$	[Xe]5d
Ce	[Xe]4f	[Xe]$5f^2$
Pr	[Xe]$4f^2$	[Xe]$4f^3$
Nd	[Xe]$4f^3$	[Xe]$4f^4$
Pm	[Xe]$4f^4$	[Xe]$4f^5$
Sm	[Xe]$4f^5$	[Xe]$4f^6$
Eu	[Xe]$4f^6$	[Xe]$4f^7$
Gd	[Xe]$4f^7$	[Xe]$4f^7$5d
Tb	[Xe]$4f^8$	[Xe]$4f^9$
Dy	[Xe]$4f^9$	[Xe]$4f^{10}$
Ho	[Xe]$4f^{10}$	[Xe]$4f^{11}$
Er	[Xe]$4f^{11}$	[Xe]$4f^{12}$
Tm	[Xe]$4f^{12}$	[Xe]$4f^{13}$
Yb	[Xe]$4f^{13}$	[Xe]$4f^{14}$
Lu	[Xe]$4f^{14}$	[Xe]$4f^{14}$7s

The Gibbs free energies of reaction (ΔG_{rxn}) for the $[Ln(NO_3)]^{2+}$ complexes are calculated with the proposed methods described in the Methods section [namely CCSD(T)-FSI/cc-pVTZ-DK3, MP2-FSI/cc-pVTZ-DK3, CCSD(T)-FSII/cc-pwCVTZ-DK3, MP2-FSI/cc-pV∞Z-DK3, CCSD(T)-FSI/cc-pV∞Z-DK3, and CCSD(T)-FSII/cc-pwCV∞Z-DK3]. The predicted ΔG_{rxn} of the $[Ln(NO_3)]^{2+}$ compounds for the lanthanoid series calculated by these methods are shown by Figure 1. All predicted ΔG_{rxn} are tabulated in Table S1 in the Supporting Information.

To assess the chemical accuracy of the computational methods used, the differences of the predicted ΔG_{rxn} with each method are compared among the options studied. Accuracy between the MP2 and CCSD(T) methods is shown by comparing the difference in the predicted ΔG_{rxn}, calculated with the CCSD(T)-FSI/cc-pVTZ-DK3 and MP2-FSI/cc-pVTZ-DK3 along with the difference between predicted ΔG_{rxn} with CCSD(T)-FSI/cc-pV∞Z-DK3 and MP2-FSI/cc-pV∞Z-DK3. Throughout the lanthanoid series, the differences in predicted ΔG_{rxn} between MP2-FSI and CCSD(T)-FSI are all under 15 kcal mol^{-1}, except for $[Nd(NO_3)]^{2+}$, [Er-

DOI: 10.1021/acsomega.8b02403
ACS Omega 2019, 4, 1375−1385

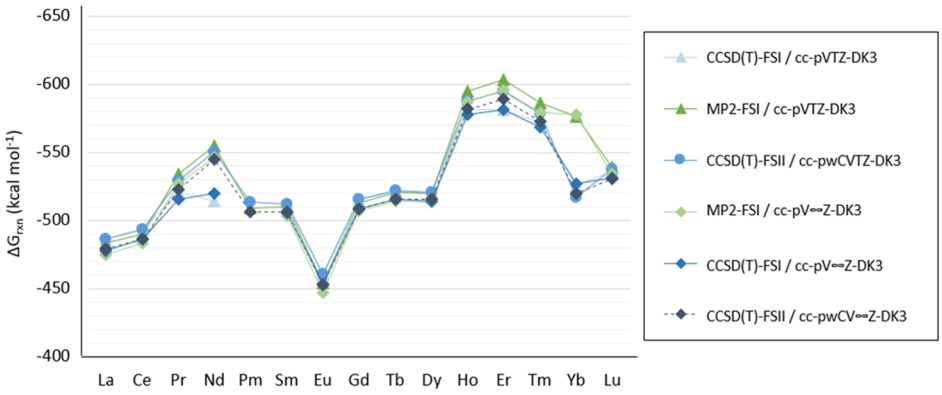

Figure 1. Predicted Gibbs free energies of reaction (ΔG_{rxn}) for the $[Ln(NO_3)]^{2+}$ complexes calculated with CCSD(T)-FSI/cc-pVTZ-DK3, MP2-FSI/cc-pVTZ-DK3, CCSD(T)-FSII/cc-pwCVTZ-DK3, MP2-FSI/cc-pV∞Z-DK3, CCSD(T)-FSI/cc-pV∞Z-DK3, and CCSD(T)-FSII/cc-pwCV∞Z-DK3.

$(NO_3)]^{2+}$, and $[Yb(NO_3)]^{2+}$ compounds, where the difference in predicted ΔG_{rxn} is 40.0, 21.8, and 50.5 kcal mol^{-1}, respectively. Using the cc-pVTZ-DK3 and cc-pV∞Z-DK3, basis sets show little effect in the difference in predicted ΔG_{rxn} between MP2-FSI and CCSD(T)-FSI except for $[Nd(NO_3)]^{2+}$ and $[Er(NO_3)]^{2+}$ for which utilizing the cc-pV∞Z-DK3 basis set showed a decrease of 13.5 and 8.0 kcal mol^{-1}, respectively.

The predicted ΔG_{rxn} obtained with CCSD(T)-FSI/cc-pVTZ-DK3 and CCSD(T)-FSII/cc-pCVTZ-DK3 are compared with those calculated with CCSD(T)-FSI/cc-pV∞Z-DK3 and CCSD(T)-FSII/cc-pwCV∞Z-DK3 to show the effects of outer-core electron correlation to the predicted ΔG_{rxn}. These effects on the predicted ΔG_{rxn} are under 10 kcal mol^{-1} throughout the lanthanoid series with $[Nd(NO_3)]^{2+}$ and $[Er(NO_3)]^{2+}$ being the only compounds for which the difference is over 10 kcal mol^{-1}. The differences in ΔG_{rxn} between considering an FSI and FSII level at the CBS limit and at the triple-ζ basis set level were similar except for $[Nd(NO_3)]^{2+}$ and $[Er(NO_3)]^{2+}$, where predicted ΔG_{rxn} from the CBS limit decrease by 11.5 and 5.9 kcal mol^{-1}, respectively.

Overall, all of the ab initio methods predict the same binding trends for the $[Ln(NO_3)]^{2+}$ complexes throughout the series, except for Nd with CCSD(T)-FSI/cc-pVTZ-DK3 and CCSD(T)-FSI/cc-pV∞Z-DK3 which show a slight increase (of about 5 kcal mol^{-1}) to the ΔG_{rxn} from $[Pr(NO_3)]^{2+}$ to $[Nd(NO_3)]^{2+}$, whereas all other methods show a decrease of about 20 kcal mol^{-1}.

Throughout the lanthanoid series, the lanthanoid in the $[Ln(NO_3)]^{2+}$ compound has been shown to have an Ln IV configuration except for Yb in which the predicted ground state has a Yb III configuration, where Yb has a fully occupied 4f shell (instead of a partly filled shell with 13 f electrons as in the Yb IV configuration). Because the Yb 4f shell is closed in this configuration, the open shell electron is in an N−O orbital. All of the computational methods tested for the proposed system in this study predict Yb III to be lower in energy except with CCSD(T)-FSI/cc-pVTZ-DK3 which predicts the Yb IV configuration to be 2.1 kcal mol^{-1} higher in energy than Yb III configuration. The CCSD(T)-FSII/cc-pwCVTZ-DK3 and CCSD(T)-FSI/cc-pV∞Z-DK3 methods predict the Yb III configuration to be 1.1 and 4.5 kcal mol^{-1} lower, respectively. The target method, CCSD(T)-FSII/cc-pwCV∞Z-DK3, shows that the Yb III configuration is more stable by 9.6 kcal mol^{-1}. The MP2 methods show a wider gap between the two configurations, where MP2-FSI/cc-pVTZ and MP2-FSI/cc-pV∞Z-DK3 show that the Yb III configuration is more stable by having a lower energy by 52.0 and 59.9 kcal mol^{-1}, respectively. A recent study on $[An(NO_3)]^{2+}$ compounds where An = Ac−Lr has also shown a ground state of an An III configuration instead of a An IV configuration for Fm, Md, and No atoms in the gas phase (but Fm IV and Md IV in the aqueous phase).[6]

COMPOSITE RESULTS

The ΔG_{rxn} for $[La(NO_3)]^{2+}$, $[Ce(NO_3)]^{2+}$, $[Pr(NO_3)]^{2+}$, $[Sm(NO_3)]^{2+}$, and $[Lu(NO_3)]^{2+}$ is calculated with the composite methods described in eq 4 (*f*-ccCA), eq 5 (method A), and eq 6 (method B). Table 2 shows the difference between the predicted ΔG_{rxn} calculated with the *f*-ccCA method and the target method [CCSD(T)-FSII/cc-pwCV∞Z-DK3+SO]. In this case, the target method contains an SO correction calculated as indicated in the ΔE_{spin}[33] correction included in *f*-ccCA.[9] The difference between the predicted ΔG_{rxn} calculated utilizing the *f*-ccCA method (for the enthalpy calculation) and the target method is shown to be small, between 0.10 and 1.21 kcal mol^{-1} throughout the $[La(NO_3)]^{2+}$, $[Ce(NO_3)]^{2+}$, $[Pr(NO_3)]^{2+}$, $[Sm(NO_3)]^{2+}$, and $[Lu(NO_3)]^{2+}$ compounds tested. The breakdown of the contribution to the predicted energy with *f*-ccCA and with the target methodology is shown in Figure 2.

Table 2. Relative Energy of $[La(NO_3)]^{2+}$, $[Gd(NO_3)]^{2+}$, and $[Lu(NO_3)]^{2+}$ ($\Delta(\Delta G)_{rxn}$) Calculated with Method A and B, Relative to CCSD(T)-FSII/cc-pwCV∞Z-DK3 and Associated Relative Computational Cost[a]

	method A $E_{ref}[MP2] + \Delta E_{CC} + \Delta E_{CV}$		method B $E_{ref}[CCSD(T)] + \Delta E_{CV}$	
	$\Delta(\Delta G)_{rxn}$ (kcal mol^{-1})	relative cost (%)	$\Delta(\Delta G)_{rxn}$ (kcal mol^{-1})	relative cost (%)
La	0.11	10	0.32	25
Gd	−0.21	10	−0.30	34
Lu	−0.44	11	−0.21	70

[a]Relative computational cost is shown as a percentage and it is calculated as relative cost = (CPU hours with method A or B)/(CPU hours with CCSD(T)-FSII/cc-pwCV∞Z-DK3) × 100; $\Delta(\Delta G)_{rxn}$ = ΔG_{rxn}(method A or B) − ΔG_{rxn}(CCSD(T)-FSII/cc-pwCV∞Z-DK3).

Moreover, the SO contribution to the overall ΔG_{rxn}, as described by the ΔE_{spin} term in *f*-ccCA, is found to be very small, under 0.49 kcal mol^{-1}, except for $[Pr(NO_3)]^{2+}$, where

DOI: 10.1021/acsomega.8b02403
ACS Omega 2019, 4, 1375−1385

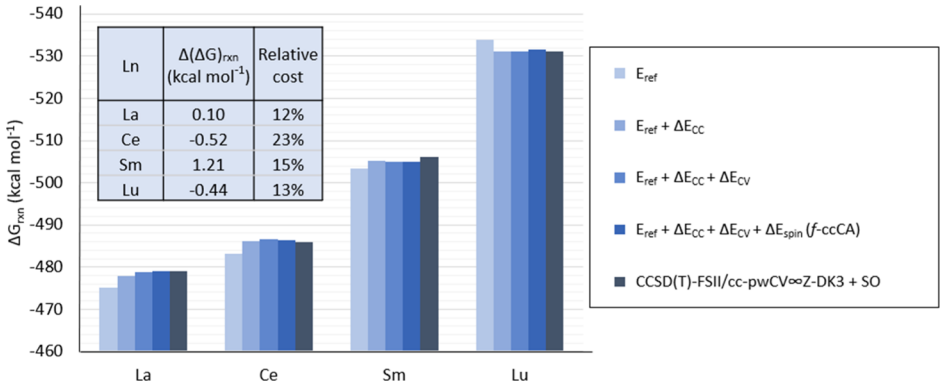

Figure 2. Predicted ΔG_{rxn} for $[Ln(NO_3)]^{2+}$ calculated with *f*-ccCA and target method [CCSD(T)-FSII/cc-pwCV∞Z-DK3 + SO]. The contribution from each term in the *f*-ccCA formulation [E_{ref}, $E_{ref} + \Delta E_{cc}$, $E_{ref} + \Delta E_{cc} + \Delta E_{cv}$, and $E_{ref} + \Delta E_{cc} + \Delta E_{cv} + \Delta E_{spin}$] is also shown. The relative computational cost and difference in predicted ΔG_{rxn} calculated with *f*-ccCA and the target method is shown in the table (inset). [Relative computational cost is shown as a percentage and it is calculated as relative cost = (CPU units with *f*-ccCA)/(CPU units with target method) × 100; $\Delta(\Delta G)_{rxn} = \Delta G_{rxn}$(*f*-ccCA) − ΔG_{rxn}(target method)].

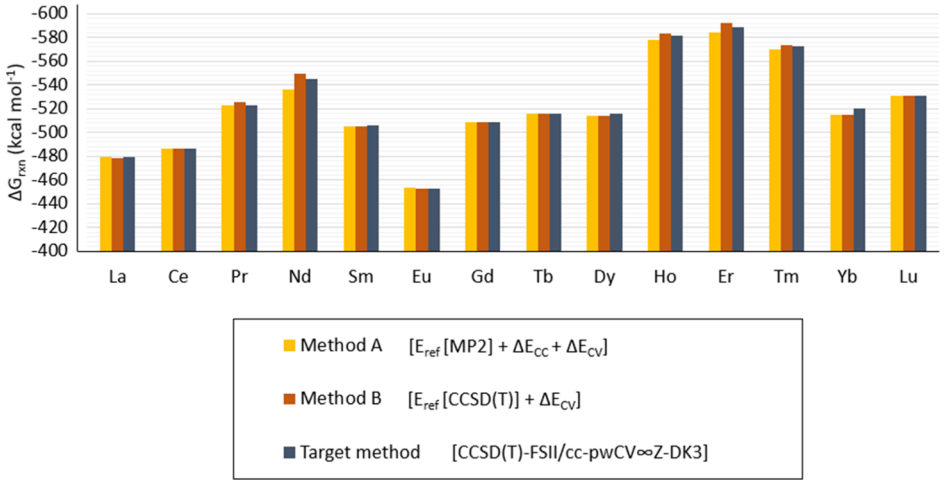

Figure 3. Predicted ΔG_{rxn} for $[Ln(NO_3)]^{2+}$ calculated with composite method A (eq 5) and method B (eq 6), along with the target method [CCSD(T)-FSII/cc-pwCV∞Z-DK3].

this contribution is predicted to be 3.8 kcal mol^{-1}. The predicted ΔG_{rxn} obtained with the composite methods A and B does not include corrections for SO coupling because it was shown that the SO correction for the reaction proposed in eq 1 is under 3 kcal mol^{-1} and therefore, incurring the additional computational cost for adding this term for the reaction was unnecessary. In method A, the reference energy is obtained at the MP2-FSI level; a higher dynamic electronic correlation term, ΔE_{cc}, is added to the CCSD(T)-FSI level; an additional outer-core electron correlation term, ΔE_{cv}, is obtained at the CCSD(T)-FSII level, which is similar to *f*-ccCA except for the inclusion of SO effects. For the composite method B, the ΔE_{cc} term is removed and the reference energy is computed at the CCSD(T)-FSI level which does not affect the ΔE_{cv} term with CCSD(T)-FSII. Predicted ΔG_{rxn} calculated with method A and method B is shown in Figure 3 for all of the lanthanoid compounds which shows a similar trend between ΔG_{rxn} and the target method, CCSD(T)-FSII/cc-pwCV∞Z-DK3 (without SO), across the lanthanoid series.

The predicted ΔG_{rxn} with *f*-ccCA (eq 4) is within 2 kcal mol^{-1} from the ΔG_{rxn} predicted with the target (CCSD(T)-FSII/cc-pwCV∞Z-DK3+SO) except for $[Nd(NO_3)]^{2+}$ where the difference is 8.6 kcal mol^{-1}. The difference between the predicted ΔG_{rxn} calculated with the composite methods from method A (eq 5) and B (eq 6) are shown to be small, under 1 kcal mol^{-1} in most of the systems, and between 3 and 13 kcal mol^{-1} for $[Nd(NO_3)]^{2+}$, $[Ho(NO_3)]^{2+}$, $[Er(NO_3)]^{2+}$, and $[Tm(NO_3)]^{2+}$. The difference between the predicted ΔG_{rxn} calculated with the composite methods described by *f*-ccCA (eq 4) with CCSD(T)-FSII/cc-pwCV∞Z-DK3+SO and CCSD(T)-FSII/cc-pwCV∞Z-DK3 (target method for *f*-ccCA, method A and method B, respectively) are shown in the Supporting Information in Table S2.

The *f*-ccCA method shows a relative computational cost between 12 and 23% for prediction of the ΔG_{rxn} of the $[Ln(NO_3)]^{2+}$ compounds over the target method [CCSD(T)-FSII/cc-pwCV∞Z-DK3+SO], as shown in Figure 2. The impact to the predicted ΔG_{rxn} is shown to be less than 1.5 kcal mol^{-1} from using *f*-ccCA. As expected, because composite method A has a reference energy computed with MP2, instead of CCSD(T), it has a lower computational cost than that when calculated with method B. Furthermore, the cost is lower (compared to the target method) for method A than for method B with less than a kcal mol^{-1} difference in the predicted ΔG_{rxn} (as shown in Table 2).

DOI: 10.1021/acsomega.8b02403
ACS Omega 2019, 4, 1375−1385

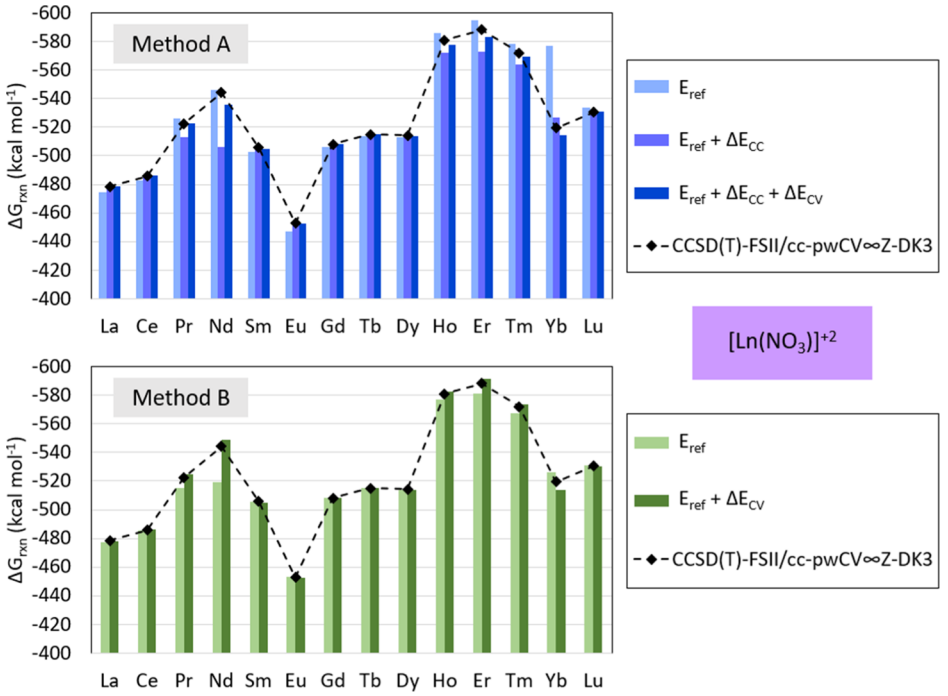

Figure 4. Predicted ΔG_{rxn} for $[Ln(NO_3)]^{2+}$ calculated with method A (top) and method B (bottom) and target method [CCSD(T)-FSII/cc-pwCV∞Z-DK3]. The contribution from each term in method A and method B formulation [E_{ref}, $E_{ref} + \Delta E_{CC}$, and $E_{ref} + \Delta E_{CC} + \Delta E_{CV}$ for method A; and E_{ref} and $E_{ref} + \Delta E_{CV}$ for method B). As indicated in eqs 5 and 6, method A is defined with E_{ref}[MP2], ΔE_{CC}[CCSD(T)], and ΔE_{CV}[CCSD(T)], and method B with E_{ref}[CCSD(T)] and ΔE_{CV}[CCSD(T)].

EVALUATION OF METHOD A AND METHOD B FOR $[LN(NO_3)]^{2+}$ AND $[LN(OH)]^{2+}$ COMPOUNDS

The predicted Gibbs free energy of reaction for $Ln(NO_3)]^{2+}$ with method A is within 0.10 and 8.59 kcal mol^{-1} from those predicted by the target method [CCSD(T)-FSII/cc-pwCV∞Z-DK3]. With method B, this difference is between 0.05 and 5.47 kcal mol^{-1}. With method A, the predicted Gibbs free energy of reaction calculated for $[La(NO_3)]^{2+}$ is 0.10 kcal mol^{-1} higher than predicted with the target method, 0.52 kcal mol^{-1} lower for $Ce(NO_3)]^{2+}$, 0.25 kcal mol^{-1} lower for $[Pr(NO_3)]^{2+}$, 8.59 kcal mol^{-1} higher for $[Nd(NO_3)]^{2+}$, 1.21 kcal mol^{-1} higher for $[Sm(NO_3)]^{2+}$, 0.29 kcal mol^{-1} lower for $[Eu(NO_3)]^{2+}$, 0.21 kcal mol^{-1} lower for $Gd(NO_3)]^{2+}$, 0.10 kcal mol^{-1} lower for $Tb(NO_3)]^{2+}$, 0.65 kcal mol^{-1} higher for $Dy(NO_3)]^{2+}$, 3.24 kcal mol^{-1} higher for $[Ho(NO_3)]^{2+}$, 4.97 kcal mol^{-1} higher for $[Er(NO_3)]^{2+}$, 2.30 kcal mol^{-1} higher for $[Tm(NO_3)]^{2+}$, 5.11 kcal mol^{-1} higher for $[Yb(NO_3)]^{2+}$, and 0.44 kcal mol^{-1} lower for $[Lu(NO_3)]^{2+}$. Comparably, with method B, the predicted Gibbs free energy of reaction calculated for $[La(NO_3)]^{2+}$ is 0.32 kcal mol^{-1} higher than predicted with the target method, 0.44 kcal mol^{-1} lower for $[Ce(NO_3)]^{2+}$, 2.47 kcal mol^{-1} lower for $[Pr(NO_3)]^{2+}$, 4.99 kcal mol^{-1} lower for $[Nd(NO_3)]^{2+}$, 0.79 kcal mol^{-1} higher for $[Sm(NO_3)]^{2+}$, 0.05 kcal mol^{-1} lower for $[Eu(NO_3)]^{2+}$, 0.30 kcal mol^{-1} lower for $[Gd(NO_3)]^{2+}$, 0.30 kcal mol^{-1} lower for $[Tb(NO_3)]^{2+}$, 0.56 kcal mol^{-1} higher for $Dy(NO_3)]^{2+}$, 1.39 kcal mol^{-1} lower for $[Ho(NO_3)]^{2+}$, 3.08 kcal mol^{-1} lower for $[Er(NO_3)]^{2+}$, 1.38 kcal mol^{-1} lower for $[Tm(NO_3)]^{2+}$, 5.47 kcal mol^{-1} higher for $[Yb(NO_3)]^{2+}$, and 0.21 kcal mol^{-1} lower for $[Lu(NO_3)]^{2+}$. These results are shown in Figure 4 and Table 3.

The calculated Gibbs free energy of reaction with method A for $[Ln(OH)]^{2+}$ is within 0.08 and 7.54 kcal mol^{-1} from those predicted by the target method [CCSD(T)-FSII/cc-pwCV∞Z-DK3] and between 0.07 and 4.57 kcal mol^{-1} with method B. The predicted Gibbs free energy of reaction calculated with method A for $[La(OH)]^{2+}$ is 1.41 kcal mol^{-1} higher than predicted with the target method, 7.54 kcal mol^{-1} higher for $[Ce(OH)]^{2+}$, 1.14 kcal mol^{-1} higher for $[Eu(OH)]^{2+}$, 1.28 kcal mol^{-1} higher for $[Gd(OH)]^{2+}$, 2.44 kcal mol^{-1} higher for $[Tb(OH)]^{2+}$, 1.38 kcal mol^{-1} higher for $[Dy(OH)]^{2+}$, 4.29 kcal mol^{-1} higher for $[Tm(OH)]^{2+}$, 0.08 kcal mol^{-1} higher for $[Yb(OH)]^{2+}$, and 1.23 kcal mol^{-1} higher for $[Lu(OH)]^{2+}$. These results are shown in Figure 5 and Table 4. Similarly, the predicted Gibbs free energy of reaction for $[Ln(OH)]^{2+}$ calculated with method B is within 0.10 and 8.59 kcal mol^{-1} from those predicted by the target method

Table 3. Predicted $\Delta(\Delta G)_{rxn}$ for $[Ln(NO_3)]^{2+}$ Calculated with Method A and Method B with Respect to the Target Method [CCSD(T)-FSII/cc-pwCV∞Z-DK3]

	method A	method B
La	0.10	0.32
Ce	−0.52	−0.44
Pr	−0.25	−2.47
Nd	8.59	−4.99
Sm	1.21	0.79
Eu	−0.29	−0.05
Gd	−0.21	−0.30
Tb	−0.10	−0.30
Dy	0.65	0.56
Ho	3.24	−1.39
Er	4.97	−3.08
Tm	2.30	−1.38
Yb	5.11	5.47
Lu	−0.44	−0.21

DOI: 10.1021/acsomega.8b02403
ACS Omega 2019, 4, 1375−1385

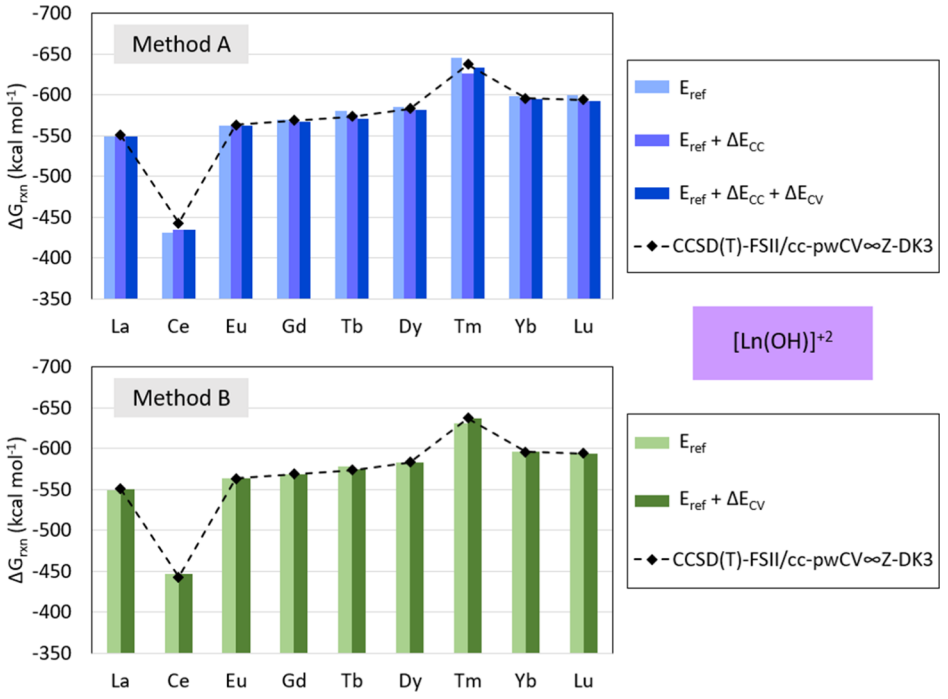

Figure 5. Predicted ΔG_{rxn} for $[Ln(OH)]^{2+}$ calculated with method A (top) and method B (bottom) and target method [CCSD(T)-FSII/cc-pwCV∞Z-DK3]. The contribution from each term in method A and method B formulation [E_{ref}, $E_{ref} + \Delta E_{CC}$, $E_{ref} + \Delta E_{CC} + \Delta E_{CV}$ for method A; and E_{ref}, $E_{ref} + \Delta E_{CV}$ for method B) are calculated as indicated in eqs 5 and 6. Method A is defined with E_{ref}[MP2], ΔE_{CC}[CCSD(T)], and ΔE_{CV}[CCSD(T)], and method B with E_{ref}[CCSD(T)] and ΔE_{CV}[CCSD(T)]. (Note Yb is in a Yb III state).

Table 4. Predicted $\Delta(\Delta G)_{rxn}$ for $[Ln(OH)]^{2+}$ Calculated with Method A and Method B with Respect to the Target Method [CCSD(T)-FSII/cc-pwCV∞Z-DK3]

	method A	method B
La	1.41	0.43
Ce	7.54	−4.57
Eu	1.14	−0.11
Gd	1.28	−0.09
Tb	2.44	−0.44
Dy	1.38	−0.32
Tm	4.29	0.24
Yb	0.80	−0.79
Lu	1.23	0.07

[CCSD(T)-FSII/cc-pwCV∞Z-DK3] and is shown in Figure 5 and Table 4. The predicted Gibbs free energy of reaction with method B for $[La(OH)]^{2+}$ is 0.43 kcal mol^{-1} higher than predicted with the target method, 4.57 kcal mol^{-1} lower for $[Ce(OH)]^{2+}$, 0.11 kcal mol^{-1} lower for $[Eu(OH)]^{2+}$, 0.09 kcal mol^{-1} lower for $[Gd(OH)]^{2+}$, 0.44 kcal mol^{-1} lower for $[Tb(OH)]^{2+}$, 0.32 kcal mol^{-1} lower for $[Dy(OH)]^{2+}$, 0.24 kcal mol^{-1} higher for $[Tm(OH)]^{2+}$, 0.74 kcal mol^{-1} lower for $[Yb(OH)]^{2+}$, and 0.07 kcal mol^{-1} higher for Lu.

COMPARISON OF METHOD A AND METHOD B

A direct comparison of predicted Gibbs free energies of reaction calculated with method A and method B is performed for $[Ln(NO_3)]^{2+}$ and $[Ln(OH)]^{2+}$ (with Ln = La, Ce, Eu, Gd, Tb, Dy, Tm, Yb, and Lu). Although the complete lanthanoid series is evaluated with method A and method B for $[Ln(NO_3)]^{2+}$, only compounds with La, Ce, Eu, Gd, Tb, Dy, Tm, Yb, and Lu are included in this discussion because of $[Ln(OH)]^{2+}$ with Ln = Pr, Nd, Sm, Ho, and Er being unavailable.

When considering all compounds included in this evaluation, on average method A and method B predict Gibbs free energies of reaction 1.73 and 0.89 kcal mol^{-1} from those calculated with the target method [CCSD(T)-FSII/cc-pwCV∞Z-DK3], respectively. The range with method B is approximately 2 kcal mol^{-1} smaller than that with method A (with method A predicting Gibbs free energies of reaction between 0.10 and 1.73 kcal mol^{-1} from the target method, and method B between 0.05 and 5.47 kcal mol^{-1}), as shown in Table 5.

Method B predicts Gibbs free energies of reaction within 1.4 kcal mol^{-1} from those predicted with the target method for all compounds in this analysis except for $[Yb(NO_3)]^{2+}$ and $[Ce(OH)]^{2+}$ with differences of 5.47 and 4.57 kcal mol^{-1}. For the same compounds, method A predicts Gibbs free energies of reaction within 4.3 kcal mol^{-1}, except for $[Yb(NO_3)]^{2+}$ and $Ce(OH)]^{2+}$ for which the differences are 5.1 and 7.5 kcal mol^{-1}, respectively. Absolute differences are shown in Table 5.

In general, Gibbs free energies of reaction calculated with method B are closer to those predicted with the target method than when calculated with method A, as shown in Table 5, Figures 6, and 7. Also, the predicted Gibbs free energies of reaction calculated with method B are often higher than those predicted with the target method, whereas those predicted with method A are often lower than those predicted by the target method. As shown in Figure 6, the predicted Gibbs free energy of reaction of $[Ln(NO_3)]^{2+}$ calculated with method A is less than 0.65 kcal mol^{-1} for all compounds in this analysis except for $[Tm(NO_3)]^{2+}$ and $[Yb(NO_3)]^{2+}$, which have a predicted energy 2.30 and 5.11 kcal mol^{-1} higher than the target method, respectively, whereas with method B the predicted Gibbs free energies are all within 0.56 kcal mol^{-1}

DOI: 10.1021/acsomega.8b02403
ACS Omega 2019, 4, 1375−1385

Table 5. Absolute Difference between ΔG_{rxn} Calculated with Method A and Method B w.r.t. the Target Method [CCSD(T)-FSII/cc-pwCV∞Z-DK3] Evaluated for All Compounds Tested in the Comparison Study [i.e., $Ln(NO_3)]^{2+}$ and $Ln(OH)]^{2+}$ (with Ln = La, Ce, Eu, Gd, Tb, Dy, Tm, Yb, and Lu)][a]

	method A		method B	
	$[Ln(NO_3)]^{2+}$	$[Ln(OH)]^{2+}$	$[Ln(NO_3)]^{2+}$	$[Ln(OH)]^{2+}$
		(a)		
La	0.10	1.41	0.32	0.43
Ce	0.52	7.54	0.44	4.57
Eu	0.29	1.14	0.05	0.11
Gd	0.21	1.28	0.30	0.09
Tb	0.10	2.44	0.30	0.44
Dy	0.65	1.38	0.56	0.32
Tm	2.30	4.29	1.38	0.24
Yb	5.11	0.80	5.47	0.79
Lu	0.44	1.23	0.21	0.07
average	1.08	2.39	1.00	0.78
range	5.01	6.74	5.42	4.50
		method A		method B
		(b)		
average		1.73		0.89
range		7.45		5.42

[a]Results shown per compound (a) and overall compounds per method (b) are in kcal mol^{-1}.

from those predicted with the target method except for $[Tm(NO_3)]^{2+}$ and $[Yb(NO_3)]^{2+}$ which have a predicted energy 1.38 kcal mol^{-1} lower and 5.47 kcal mol^{-1} higher than the target method, respectively. The Gibbs free energy of reaction of the $[Ln(OH)]^{2+}$ compounds calculated with method A is between 0.80 and 7.54 kcal mol^{-1} higher than those predicted with the target method, whereas when calculated with method B, all predicted Gibbs free energies are within 0.79 kcal mol^{-1} from those predicted by the target method, except for $[Ce(NO_3)]^{2+}$ with a predicted ΔG_{rxn} 4.57 kcal mol^{-1} lower than predicted by the target method. All values are shown in Figures 6 and 7.

CONCLUSIONS

Computational predictive capabilities are essential to optimize the design of ligands for selective binding of lanthanoids. In particular, cost-efficient methods are critical for industrial applications, as processes at industrial scales can greatly benefit from robust and efficient computational protocols. In this study, the Gibbs free energy of reaction of a nitrate ion bound to lanthanoid ions is calculated with ab initio methods including CCSD(T) and composites. Finding computationally efficient methods for predictive capabilities of nitrate ligands bound to lanthanoids is essential because of the importance of nitric acid use in the separation process and subsequent nitrate complexation to lanthanoids.

The SO contribution to the proposed reaction is small (less than 0.45 kcal mol^{-1}) for the compounds tested, and therefore found unnecessary in the evaluation of the Gibbs free energy in the studied binding reaction. All lanthanoid ions in this study presented a behavior corresponding to an Ln IV configuration except for Yb, which presented a Yb III configuration similar to No in previous studies of actinoid nitrate systems (following the NIST nomenclature indicated in Table 1). The effects of higher electron correlation beyond MP2 ranges from 2 to 50 kcal mol^{-1} through the lanthanoid series, whereas the effects of outer-core correlation are less than 10 kcal mol^{-1} (except for Nd and Eu, where it is 24.6 and 7.2 kcal mol^{-1}, respectively). All composites included in this study predict Gibbs free energies of reaction within approximately 3 kcal mol^{-1} from each other at a fraction of the cost of the target methodology [CCSD(T)-FSII/cc-pwCV∞Z-DK3 for method A and B, and CCSD(T)-FSII/cc-pwCV∞Z-DK3+SO for *f*-ccCA]. The composite method A [where E_{ref} is described by MP2] predicts Gibbs free energies of reaction between 0.09 and 8.59 kcal mol^{-1} from those predicted by the target method at a computational cost between 10 and 32% of the target method. The Gibbs free energy predicted utilizing *f*-ccCA between 0.11 and 1.21 kcal mol^{-1} from those predicted by the target method at a computational cost between 12 and 23% of the target method. The Gibbs free energy of reaction predicted with the composite method B (where E_{ref} is described by CCSD(T)) is between 0.05 and 5.47 kcal mol^{-1} from those predicted by the target method at a computational cost between 22 and 70% of the target method.

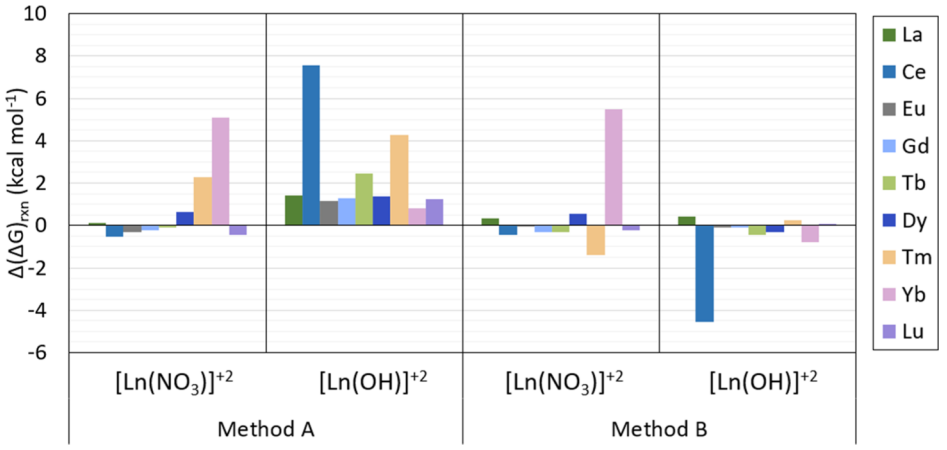

Figure 6. Difference between ΔG_{rxn} calculated with method A and method B w.r.t. the target method [CCSD(T)-FSII/cc-pwCV∞Z-DK3] evaluated for all compounds tested in the comparison study (that is, $Ln(NO_3)]^{2+}$ and $Ln(OH)]^{2+}$ (with Ln = La, Ce, Eu, Gd, Tb, Dy, Tm, Yb, and Lu)). Results shown are in kcal mol^{-1}.

DOI: 10.1021/acsomega.8b02403
ACS Omega 2019, 4, 1375−1385

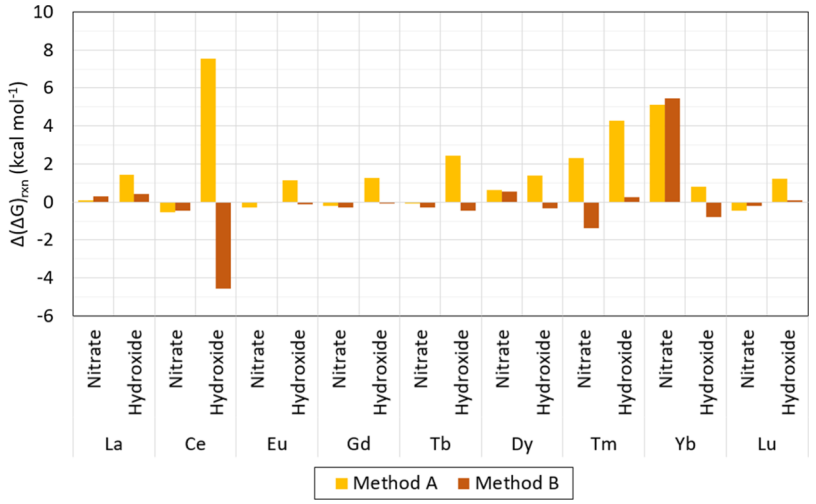

Figure 7. Difference between ΔG_{rxn} calculated with method A and method B w.r.t. the target method [CCSD(T)-FSII/cc-pwCV∞Z-DK3] evaluated for all compounds tested in the comparison study (i.e., $Ln(NO_3)]^{2+}$ and $Ln(OH)]^{2+}$ (with Ln = La, Ce, Eu, Gd, Tb, Dy, Tm, Yb, and Lu)). Results shown are in kcal mol^{-1}.

This study provides options for ab initio methods that can predict Gibbs free energies of reaction for the binding of nitrates to lanthanoids at a lower computational cost than CCSD(T). Although the focus of the study is on $[Ln(NO_3)]^{2+}$, the proposed method A and method B are also evaluated on $[Ln(OH)]^{2+}$, showing promising future extensions of these methods to other lanthanoid-containing compounds. Future work will include expanding the application of these methods to fully complexed systems of interest in separation technologies.

■ ASSOCIATED CONTENT

Supporting Information

The Supporting Information is available free of charge on the ACS Publications website at DOI: 10.1021/acsomega.8b02403.

Predicted Gibbs free energy of reaction for $[Ln(NO_3)]^{2+}$ calculated with CCSD(T)-FSI/cc-pVTZ-DK3, MP2-FSI/cc-pVTZ-DK3, CCSD(T)-FSII/cc-pwCVTZ-DK3, MP2-FSI/cc-pV∞Z, CCSD(T)-FSI/cc-pV∞Z-DK3, and CCSD(T)-FSII/cc-pwCV∞Z-DK3; method A and method B described in the Methods section; and relative computational cost (PDF)

■ AUTHOR INFORMATION

Corresponding Authors

*E-mail: dpenchof@utk.edu (D.A.P.).
*E-mail: hhall6@utk.edu (H.L.H.).

ORCID

Deborah A. Penchoff: 0000-0002-7430-9452

Notes

The authors declare no competing financial interest.

■ ACKNOWLEDGMENTS

This work was supported in part by the National Nuclear Security Administration (grant DOE-NNSA-DE-NA0001983) under the Stewardship Science Academic Alliance Program (D.A.P., J.D.A., and H.L.H.). D.A.P. thanks Dr. J. F. Corbey and Dr. M. T. Cook for useful discussions. The views expressed here are those of the authors and do not necessarily reflect those of NNSA. Computational resources were provided by UNT's High Performance Computing Services, a division of the University Information Technology with additional support from UNT Office of Research and Economic Development. This material is based upon work performed using computational resources supported by the University of Tennessee and Oak Ridge National Laboratory Joint Institute for Computational Sciences (http://www.jics.tennessee.edu). This work used the Extreme Science and Engineering Discovery Environment (XSEDE),[44] which is supported by National Science Foundation grant number ACI-1548562. This research used resources of the National Energy Research Scientific Computing Center, a DOE Office of Science User Facility supported by the Office of Science of the U.S. Department of Energy under Contract no. DE-AC02-05CH11231. The *f*-ccCA[9] methodology has been included in full or in part in presentations at American Chemical Society Meetings,[45] among other professional meetings.

■ REFERENCES

(1) Mincher, B. J.; Modolo, G.; Mezyk, S. P. Review Article: The Effects of Radiaton Chemistry on Solvent Extraction: 2. A Review of Fission-Product Extraction. *Solvent Extr. Ion Exch.* **2009**, *27*, 331−353.

(2) Corbey, J. F.; Rapko, B. M.; Wang, Z.; McNamara, B. K.; Surbella, R. G.; Pellegrini, K. L.; Schwantes, J. M. Crystallographic and Spectroscopic Characterization of Americium Complexes Containing the Bis[(Phosphino)Methyl]Pyridine-1-Oxide (NOPOPO) Ligand Platform. *Inorg. Chem.* **2018**, *57*, 2278−2287.

(3) Rosario-Amorin, D.; Ouizem, S.; Dickie, D. A.; Wen, Y.; Paine, R. T.; Gao, J.; Grey, J. K.; de Bettencourt-Dias, A.; Hay, B. P.; Delmau, L. H. Synthesis, Lanthanide Coordination Chemistry, and Liquid-Liquid Extraction Performance of CMPO-Decorated Pyridine and Pyridine N-Oxide Platforms. *Inorg. Chem.* **2013**, *52*, 3063−3083.

(4) Tian, G.; Shuh, D. K.; Beavers, C. M.; Teat, S. J. A Structural and Spectrophotometric Study on the Complexation of Am(III) with TMOGA in Comparison with the Extracted Complex of DMDOOGA. *Dalton Trans.* **2015**, *44*, 18469−18474.

(5) Hirshorn, S. R. *NASA System Engineering Handbook*, 2nd ed.; National Aeronautics and Space Administration: Washington, DC, 2007.

(6) Penchoff, D. A.; Peterson, C. C.; Quint, M. S.; Auxier, J. D.; Schweitzer, G. K.; Jenkins, D. M.; Harrison, R. J.; Hall, H. L.

DOI: 10.1021/acsomega.8b02403
ACS Omega 2019, 4, 1375−1385

Structural Characteristics, Population Analysis, and Binding Energies of $[An(NO_3)]^{2+}$ [with An = Ac - Lr]. *ACS Omega* **2018**, *3*, 14127−14143.
(7) Szabo, A.; Ostlund, N. S. *Modern Quantum Chemistry*, 1st ed.; Dover Publications, Inc.: Mineola, NY, 1982.
(8) Jensen, F. Relativistic Methods. *Introduction to Computational Chemistry*; John Wiley & Sons: West Sussex, England, 2007; pp 277−292.
(9) Peterson, C. C. *Accurate Energetics Across the Periodic Table Via Quantum Chemistry*; University of North Texas, 2015.
(10) DeYonker, N. J.; Cundari, T. R.; Wilson, A. K. The Correlation Consistent Composite Approach (CcCA): An Alternative to the Gaussian-n Methods. *J. Chem. Phys.* **2006**, *124*, 114104.
(11) Peterson, C.; Penchoff, D. A.; Wilson, A. K. *Prediction of Thermochemical Properties Across the Periodic Table: A Review of the Correlation Consistent Composite Approach (CcCA) Strategies and Applications*, 2016.
(12) Lu, Q.; Peterson, K. A. Correlation Consistent Basis Sets for Lanthanides: The Atoms La-Lu. *J. Chem. Phys.* **2016**, *145*, 054111.
(13) Solomonik, V. G.; Smirnov, A. N. Toward Chemical Accuracy in Ab Initio Thermochemistry and Spectroscopy of Lanthanide Compounds: Assessing Core−Valence Correlation, Second-Order Spin−Orbit Coupling, and Higher Order Effects in Lanthanide Diatomics. *J. Chem. Theory Comput.* **2017**, *13*, 5240.
(14) Madic, C.; Lecomte, M.; Baron, P.; Boullis, B. Separation of Long-Lived Radionuclides from High Active Nuclear Waste. *Compt. Rendus Phys.* **2002**, *3*, 797−811.
(15) Hudson, M.; Lewis, F.; Harwood, L. Development of Highly Selective Ligands for Separations of Actinides from Lanthanides in the Nuclear Fuel Cycle. *Synlett* **2011**, *18*, 2609−2632.
(16) Glatz, J.-P. Spent Fuel Dissolution and Reprocessing Processes. *Comprehensive Nuclear Materials*; Elsevier, 2012; pp 343−366.
(17) Diwu, J.; Wang, S.; Liao, Z.; Burns, P. C.; Albrecht-Schmitt, T. E. Cerium(IV), Neptunium(IV), and Plutonium(IV) 1,2-Phenylenediphosphonates: Correlations and Differences between Early Transuranium Elements and Their Proposed Surrogates. *Inorg. Chem.* **2010**, *49*, 10074−10080.
(18) Bond, E. M.; Duesler, E. N.; Paine, R. T.; Neu, M. P.; Matonic, J. H.; Scott, B. L. Synthesis and Molecular Structure of a Plutonium(IV) Coordination Complex: $[Pu(NO_3)_2\{2,6\text{-}[(C_6H_5)2P(O)CH_2]_2C_5H_3NO\}_2](NO_3)_2\cdot 1.5H_2O\cdot 0.5MeOH$. *Inorg. Chem.* **2000**, *39*, 4152−4155.
(19) Rapko, B. M.; Duesler, E. N.; Smith, P. H.; Paine, R. T.; Ryan, R. R. Chelating Properties of 2-((Diphenylphosphino)Methyl)-Pyridine N,P-Dioxide and 2,6-Bis((Diphenylphosphino)Methyl)-Pyridine N,P,P′-Trioxide toward f-Element Ions. *Inorg. Chem.* **1993**, *32*, 2164−2174.
(20) Whittaker, D. M.; Griffiths, T. L.; Helliwell, M.; Swinburne, A. N.; Natrajan, L. S.; Lewis, F. W.; Harwood, L. M.; Parry, S. A.; Sharrad, C. A. Lanthanide Speciation in Potential SANEX and GANEX Actinide/Lanthanide Separations Using Tetra-N-Donor Extractants. *Inorg. Chem.* **2013**, *52*, 3429−3444.
(21) Van de Voorde, M.; Van Hecke, K.; Binnemans, K.; Cardinaels, T. Separation of Samarium and Europium by Solvent Extraction with an Undiluted Quaternary Ammonium Ionic Liquid: Towards High-Purity Medical Samarium-153. *RSC Adv.* **2018**, *8*, 20077−20086.
(22) Lavrov, H. V.; Ustynyuk, N. A.; Matveev, P. I.; Gloriozov, I. P.; Zhokhov, S. S.; Alyapyshev, M. Y.; Tkachenko, L. I.; Voronaev, I. G.; Babain, V. A.; Kalmykov, S. N.; et al. A Novel Highly Selective Ligand for Separation of Actinides and Lanthanides in the Nuclear Fuel Cycle. Experimental Verification of the Theoretical Prediction. *Dalton Trans.* **2017**, *46*, 10926−10934.
(23) Muller, J. M.; Galley, S. S.; Albrecht-Schmitt, T. E.; Nash, K. L. Characterization of Lanthanide Complexes with Bis-1,2,3-Triazole-Bipyridine Ligands Involved in Actinide/Lanthanide Separation. *Inorg. Chem.* **2016**, *55*, 11454−11461.
(24) Bernstein, K. J.; Do-Thanh, C.-L.; Penchoff, D. A.; Cramer, S. A.; Murdock, C. R.; Lu, Z.; Harrison, R. J.; Camden, J. P.; Jenkins, D. M. The Synthesis and Spectroscopic Characterization of an Aromatic Uranium Amidoxime Complex. *Inorg. Chim. Acta.* **2014**, *421*, 374−379.
(25) Chen, J.; Wang, S.; Xu, C.; Wang, X.; Feng, X. Separation of Americium from Lanthanides by Purified Cyanex 301 Countercurrent Extraction in Miniature Centrifugal Contactors. *Procedia Chem.* **2012**, *7*, 172−177.
(26) Møller, C.; Plesset, M. S. Note on an Approximation Treatment for Many-Electron Systems. *Phys. Rev.* **1934**, *46*, 618−622.
(27) Cramer, C. J. *Essentials of Computational Chemistry*; Wiley, 2002.
(28) de Jong, W. A.; Harrison, R. J.; Dixon, D. A. Parallel Douglas-Kroll Energy and Gradients in NWChem: Estimating Scalar Relativistic Effects Using Douglas-Kroll Contracted Basis Sets. *J. Chem. Phys.* **2001**, *114*, 48−53.
(29) Reiher, M. *Relativistic Douglas-Kroll-Hess Theory*; Wiley Interdisciplinary Reviews: Computational Molecular Science, 2012; pp 139−149.
(30) Karton, A.; Martin, J. M. L. Comment on: "Estimating the Hartree−Fock Limit from Finite Basis Set Calculations" [Jensen F (2005) Theor Chem Acc 113:267]. *Theor. Chem. Acc.* **2006**, *115*, 330−333.
(31) Martin, J. M. L. Ab Initio Total Atomization Energies of Small Molecules — towards the Basis Set Limit. *Chem. Phys. Lett.* **1996**, *259*, 669−678.
(32) Gomes, A. S. P.; Dyall, K. G.; Visscher, L. Relativistic Double-Zeta, Triple-Zeta, and Quadruple-Zeta Basis Sets for the Lanthanides La−Lu. *Theor. Chem. Acc.* **2010**, *127*, 369−381.
(33) Peterson, C.; Penchoff, D. A.; Wilson, A. K. Ab Initio Approaches for the Determination of Heavy Element Energetics: Ionization Energies of Trivalent Lanthanides (Ln = La-Eu). *J. Chem. Phys.* **2015**, *143*, 194109.
(34) Penchoff, D. A.; Peterson, C. C.; Camden, J. P.; Bradshaw, J. A.; Auxier, J. D.; Schweitzer, G. K.; Jenkins, D. M.; Harrison, R. J.; Hall, H. L. Structural Analysis of the Complexation of Uranyl, Neptunyl, Plutonyl, and Americyl with Cyclic Imide Dioximes. *ACS Omega* **2018**, *3*, 13984−13993.
(35) Becke, A. D. Perspective: Fifty Years of Density-Functional Theory in Chemical Physics. *J. Chem. Phys.* **2014**, *140*, 18A301.
(36) Becke, A. D. Density-Functional Thermochemistry. III. The Role of Exact Exchange. *J. Chem. Phys.* **1993**, *98*, 5648−5652.
(37) Krishnan, R.; Binkley, J. S.; Seeger, R.; Pople, J. A. Self-consistent Molecular Orbital Methods. XX. A Basis Set for Correlated Wave Functions. *J. Chem. Phys.* **1980**, *72*, 650−654.
(38) Valiev, M.; Bylaska, E. J.; Govind, N.; Kowalski, K.; Straatsma, T. P.; Van Dam, H. J. J.; Wang, D.; Nieplocha, J.; Apra, E.; Windus, T. L.; et al. NWChem: A Comprehensive and Scalable Open-Source Solution for Large Scale Molecular Simulations. *Comput. Phys. Commun.* **2010**, *181*, 1477−1489.
(39) Werner, H.-J.; Knowles, P. J.; Knizia, G.; Manby, F. R.; Schütz, M. A General Purpose Quantum Chemistry Package. *Wiley Interdiscip. Rev.: Comput. Mol. Sci.* **2012**, *2*, 242−253.
(40) Bast, R.; Saue, T.; Visscher, L.; Jensen, H. J. A.; Bakken, V.; Dyall, K. G.; Dubillard, S.; Ekstroem, U.; Eliav, E.; Enevoldsen, T.; Fasshauer, E.; et al. DIRAC, a Relativistic Ab Initio Electronic Structure Program. *Realease DIRAC15*; Dirac, 2015.
(41) Feller, D. The Role of Databases in Support of Computational Chemistry Calculations. *J. Comput. Chem.* **1996**, *17*, 1571−1586.
(42) Schuchardt, K. L.; Didier, B. T.; Elsethagen, T.; Sun, L.; Gurumoorthi, V.; Chase, J.; Li, J.; Windus, T. L. Basis Set Exchange: A Community Database for Computational Sciences. *J. Chem. Inf. Model.* **2007**, *47*, 1045−1052.
(43) Kramida, A.; Ralchenko, Y.; Reader, J. .; Team, N. A. *NIST Atomic Spectra Database*. (Ver. 5.5.2), [Online], Gaithersburg, MD, 2018.
(44) Towns, J.; Cockerill, T.; Dahan, M.; Foster, I.; Gaither, K.; Grimshaw, A.; Hazlewood, V.; Lathrop, S.; Lifka, D.; Peterson, G. D.; et al. XSEDE: Accelerating Scientific Discovery. *Comput. Sci. Eng.* **2014**, *16*, 62−74.

DOI: 10.1021/acsomega.8b02403
ACS Omega 2019, 4, 1375−1385

(45) (a) Peterson, C. C.; Wilson, A. K. Ab Initio Approaches for Accurate Predictions of Lanthanide Thermochemistry. *Abstracts of Papers, 249th ACS National Meeting & Exposition*; Denver, CO, United States, 2015; PHYS-488. (b) Penchoff, D.; Peterson, C.; Schweitzer, G.; Wilson, A. Optimization of Separations of Rare Earths and Actinides through Computational Approaches. *Abstracts of Papers, 251st ACS National Meeting & Exposition*; San Diego, CA, Unites States, 2016; EC-147. (c) Penchoff, D.; Peterson, C.; Auxier, J.; Hall, H.; Wilson, A. Optimization of Selective Separations of Lanthanides: An Integrated Computational and Experimental Study. *Abstracts of Papers, 251st ACS National Meeting & Exposition*; San Diego, CA, Unites States, 2016; NUCL-126. (d) Peterson, C.; Penchoff, D.; Wilson, A. Composite Approach towards Accurate Predictions of Lanthanide and Actinide Thermochemistry. *Abstracts of Papers, 251st ACS National Meeting & Exposition*; San Diego, CA, Unites States, 2016; COMP-626. (e) Penchoff, D.; Peterson, C.; Auxier, J.; Hall, H.; Wilson, A. Improving Rapid Separations for Nuclear Forensics through Computational Techniques. *Abstracts of Papers, 252nd ACS National Meeting & Exposition*; Philadelphia, PA, Unites States, 2016; NUCL-14. (f) Penchoff, D.; Peterson, C.; Schweitzer, G.; Wilson, A. Computational Predictions for Separations of Lanthanides and Actinides. *Abstracts of Papers, 252nd ACS National Meeting & Exposition*; Philadelphia, PA, Unites States, 2016; INOR-61. (g) Peterson, C.; Penchoff, D.; Wilson, A. Composite Approaches for Accurate Predictions of Lanthanide and Actinide Chemistry. *Abstracts of Papers, 252nd ACS National Meeting & Exposition*; Philadelphia, PA, Unites States, 2016; COMP-76. (h) Penchoff, D. A.; Peterson, C.; Wilson, A. K. Thermochemical and Structural Predictions of Lanthanide- and Actinide-Containing Compounds: A Computational Perspective. *Abstracts of Papers, 253rd ACS National Meeting & Exposition*; San Francisco, CA, United States, 2017; INOR-1135.

DOI: 10.1021/acsomega.8b02403
ACS Omega 2019, 4, 1375−1385